THIRD EUROPEAN ROTORCRAFT AND POWERED LIFT AIRCRAFT FORUM

PAPER No.50

GEARBOX DYNAMICS - MODELLING OF A SPIRAL BEVEL GEARBOX

D. ASTRIDGE and M. SALZER

WESTLAND HELICOPTERS LTD.

September 7-9, 1977

AIX-EN-PROVENCE, FRANCE

ASSOCIATION AERONAUTIQUE ET ASTRONAUTIQUE DE FRANCE

GEARBOX DYNAMICS - MODELLING OF A SPIRAL BEVEL GEARBOX

D. ASTRIDGE, AND M. SALZER, WESTLAND HELICOPTERS LTD

1. INTRODUCTION

Non uniform motion in helicopter power transmission gears can result in significant limitation of overhaul life, acute crew fatigue and communications problems. It is not surprising therefore that the problem is being tackled on many fronts, sometimes with quite sophisticated tools. Westland Helicopters Ltd are attacking the problem at source (gear transmission errors and system response), noise transmission to the aircraft structure (damping and isolation), and response of the structure (structural damping and acoustic treatments) (1).

Helicopter gears are manufactured to very high standards of accuracy with close tolerances but modern NC multi axis machines and electronically controlled grinding machines offer further scope for improvement. However it is important to identify the corrections that will yield most benefit, and the critical gear meshes in a multi-mesh system. There is considerable scope for modifying the response of the gearbox to meshing error excitation, by manipulating mass and stiffness of the components themselves. This can be accomplished to a certain degree without the addition of weight, especially with new materials and production processes becoming available, but there is scope also for weight saving in gear configuration and modified tooth forms that could usefully be used to reduce noise and vibration and extend component lives.

The analysis of the dynamics of a spiral bevel gearbox described herein is a first step towards the analysis of complex main rotor gearboxes at WHL. A validated model will permit modal and forced response (axial, lateral and torsional) of the complete gearbox to a complex transmission error forcing function to be predicted at the design stage. The lumped-mass approach adopted in this model allows six degrees of freedom at a number of nodes sufficient to define the behaviour of the complete system with acceptable accuracy. The analysis provides a tractable design tool requiring straightforward digital matrix handling techniques of modest proportions and is ideal for parametric studies required to optimise component geometry, absorber design etc.

2. GEAR TRANSMISSION ERROR

The principal source of excitation in the frequency range over which the internal noise problem is most acute (500-4kHz) is non conjugate action at the mesh, or transmission error. Major contributors in helicopter gears are:-

i) manufacturing errors and tolerances on gear teeth - profile, lead and pitch

ii) stiffness variation through the mesh cycle due to bending, shear and contact deflections

iii) misalignment of gears due to deflection of shafts and casing under load and thermal expansion, and due to manufacturing and assembly errors.

Other contributors of perhaps less significance include variation of traction forces, bearing geometry, and shaft imbalance.

Deflections of gears, shafts and housings are significant in helicopter gearboxes, where high power/weight ratio is an important objective. Total deflections measured at the casing can be an order of magnitude greater than manufacturing tolerances on gear teeth. Tooth form and lead corrections can be introduced to accommodate deflection errors, but will only be correct for one load condition, and complete elimination of displacement errors is impracticable.

3. MATHEMATICAL MODELLING

Gearbox response can be modified at the development stage, but this is costly in duplication of component manufacture and testing, prolongs aircraft programmes and must therefore be very limited in scope. Development of a mathematical model is essential for optimising component geometry at the design stage.

A satisfactory dynamic model may be used:-

i) to study influence of different types of gear error

ii) to determine the most sensitive mesh in a complex gearbox

iii) to manipulate system response by adjustments to mass and stiffness distribution in components, particularly to avoid mode shapes that adversely affect gear and bearing life

iv) to determine location and effectiveness of absorbers, damping rings, etc. and undesirable side effects

v) to relate behaviour of internal components to casing vibration, as it is rarely practicable to fully instrument internal components

vi) to aid condition monitoring - (v) above plus study of changes in response due to changes in tooth profiles or stiffness simulating surface damage and cracks.

In selecting the analysis scheme for a model it is essential to obtain a reasonable balance between accuracy and economy/tractability. The simplest possible model is a single degree-of-freedom torsional model in which gears are represented by uncoupled inertias, and the mesh by a constant or time-dependent stiffness. Many of the fundamental mechanisms of gear vibration have been studied with this model (2). Such a model is useful in that non-linearities such as separation and reverse face contact may be included (3). This analysis may be readily extended (e.g.4) to include additional torsional freedoms. However, in helicopter applications where support stiffnesses are relatively low and readily couple,usefulness of torsional models is limited to low frequencies. For most of the frequency range of concern translational freedoms and reaction coupling must be introduced, either by means of lumped-mass multi-degree-of-freedom models or by finite-element models. A model figuring most prominently in the literature is that developed by Boeing Vertol/MTI (5). This comprises a three stage approach:-

i) analysis of gear error excitation

ii) application of i) to a complex torsion-only model to predict dynamic tooth loads

iii) application of ii) independently to a NASTRAN finite-element model of the shaft-bearing systems.

Modifications to an existing main rotor gearbox have been derived on the basis of this analysis. We look forward to seeing Vertol reports of the results of tests on a gearbox thus modified, which we understand were very successful in terms of noise reduction at troublesome frequencies. We are convinced that a complete solution of adequate accuracy can be obtained by a lumped-mass modelling technique however, making the three-stage approach unnecessary.

4. WHL MODEL OF A SPIRAL BEVEL GEARBOX

A single stage spiral bevel gearbox was selected for modelling in the first instance because this represents a simple form of generalized three-dimensional gearing system. Subsequent development of the analysis will involve main rotor gearboxes for which gear noise is a problem. The Wessex tail rotor gearbox (fig.1) was chosen because a test rig was available for verifying the model and a great deal of relevant experimental data existed already. From this data it was clear that shaft bending, and coupling of bearing reactions through the case must be allowed for in the model. It was also clear that a linear model would be adequate because dynamic loads were less than 10% of steady loads and fairly independent of load. This enabled cost effective standard linear algebraic techniques to be applied using digital computation.

The gearbox was idealised as shown in fig.2, mass and inertia being concentrated at 13 stations on the shafts and housing, each with six degrees-of-freedom. Ten of the stations were chosen to coincide with bearing locations where mass tends to be concentrated anyway, two were at the gear and pinion centres, and there was one additional station on the intermediate casing. The shafts and much of the casing was idealized by hollow cylindrical beams with bending and shear deflections treated. A finite-element analysis of the more complex intermediate casing was available and therefore used to obtain a stiffness matrix relating the three stations on this component. The tapered roller bearings were idealised by direct stiffness terms only but cross-stiffness data is now available for these bearings (ref.6). The tooth mesh has been modelled as a single point load normal to the central contacting surface, with magnitude proportional to the normal component of relative mesh displacement. Platform excitation was introduced at the mesh point to simulate gear transmission errors in the forced response studies. Low torsional and lateral stiffnesses were applied at the shaft extremities to simulate the rubber couplings used on the rig. The input housing was assumed to be attached to a massive inertia which again corresponds to the rig. The results were consistent with the assumptions of the idealisation, which resulted in 78 degrees of freedom for the system.

5. RESULTS

5.1. Static Deflections

The deflections predicted for the model for a steady torque of 4500 lbf-in (508 N.m) are plotted on orthogonal axes in fig.4. The results show very little relative displacements across the bearings (i.e. the shafts and casing virtually move as one), with the largest deflection being out of the plane of the shafting at the intermediate casing. Deflection measurements made on the rig correlated satisfactorily with predictions, justifying use of the predicted stiffness matrix in the dynamic analysis.

5.2. Natural Frequencies and Normal Modes

Natural frequencies and normal modes are determined by extraction of the eigenvalues and vectors of the dynamic matrix. Values of the predicted natural frequencies up to 5k.Hz are listed in table 1, together with a brief description of the mode shape. Some sample mode shapes are plotted in figs. 5-7 using the conventions of fig.3. Approximately half of the natural frequencies fall in this frequency range, but very few of these are susceptible to gear mesh excitation as indicated by the values in the fourth column of table 1.

Low frequency modes (e.g. fig.5) tend to produce simple low order bending of some components with little relative deflection of shafts and casing, negligible lateral deflection at the bearings, and small normal components of relative tooth deflection, i.e. low dynamic tooth and bearing loads. At higher frequencies mode shapes become complex, and interaction between the components becomes significant. Even so the number of frequencies at which significant normal relative displacement occurs at the gear mesh is relatively small and few of the predicted modes are likely to be excited in practice. Fig.6 shows an example (at 1047Hz) where mesh displacement is significant. Fig.7 (2297Hz) shows the complex interactions typical of the higher frequency modes, with significant axial and radial displacements across the bearings. At frequencies above 5kHz the complexity of mode shape would require a corresponding increase in complexity of the model, but the gear noise problem is limited to frequencies below this.

Comparison of results from this model with those of a torsional model of the internal components are shown in table 2. In general each torsional mode is affected by lateral displacements, resulting in two or more natural frequencies occurring near the torsional prediction. Fig.8 compares predicted torsional behaviour at frequencies near 1.5kHz.

The close gouping of natural frequencies in certain zones is noteworthy - for example the modes at 1047Hz, 1146Hz and 1282Hz all display significant deflection of the input shaft, but are distinguished by phase inversions in the input and output sections. It is important to recognise the existence of such behaviour since it could cause severe problems in the interpretation of experimental response data and the extraction of damping factors.

5.3. Forced Response - Sinusoidal Excitation

The model was evaluated with simple sinusoidal excitation of .001in (25μm) peak before introducing the complexity of gear transmission error spectra. In order to determine forced response it was necessary to make certain assumptions about damping, in view of the limited amount of measured data. It was assumed in the first instance that damping did not couple modes, and modal Q-factors between the limits 8 and 22 (based on limited measured data) were assigned with the aid of mode shape information. For instance damping in simple low order bending modes was judged to be low, whilst in modes with significant interface distortion, bearing displacements, or sliding at the gear mesh, higher damping was assumed. Assumed Q-factors are shown in table 1. Response due to the 25μm sinusoidal excitation are shown for two stations in figs.9 and 10. General features of the results include:-

i) relatively few peaks occur on any particular curve despite the existence of 33 natural frequencies in the range up to 4k.Hz. This is due to the low relative mesh normal displacement at most of the modes,

ii) troughs, or anti-resonance features, are at least as pronounced as peaks,

iii) bearing relative displacements tend to be much smaller than casing displacements. Peak values correspond to dynamic bearing loads of 700lbf (3140N) per thou (25μm) excitation,

iv) relative normal mesh displacement shows a gradual increase in magnitude with increasing frequency (fig.10), with local peaks superimposed. Above 3k.Hz peak displacements correspond to approximately 1000lbf (4448N) per thou excitation.

5.4. Forced Response - Transmission Error Spectra

Transmission error measurements on the actual gears in the rig were not available, so a forcing spectrum was derived based on pitch-error traces from similar gears and on manufacturing tolerances (AGMA10). Typical traces showed the fundamental (eccentricity) term to dominate, with consequent production of sidebands around tooth mesh frequency and harmonics. Alternate tooth spacing error variation were present, producing peaks at approximately half meshing frequency. Mesh frequency components were derived from a Fourier Analysis of a .0002in (5μm) rectified sinusoid. The resulting spectra for pinion and gear are shown in fig.11.

The response to this excitation at 2730 rpm, predicted by the model is shown in fig.12a for the casing at station 7 (out-of-shaft plane). Fig.12b shows a measured spectrum, albeit for a slightly different plane, for comparison. The precise correspondence of the frequencies arises from the excitation spectra used, but the order of magnitude agreement generally of spectral components suggests that the model is reasonably good. The significant discrepancy below 200Hz suggests inadequacy of the excitation spectra at these frequencies, and points to the need to measure in situ the transmission errors of the actual gears used. The presence of intermediate gearbox meshing frequency indicates that improved isolation is required at the coupling.

6. PARAMETRIC STUDY

Model validation tests are planned, and these should be completed before extensive parametric studies are justified. However some preliminary studies were carried out in order to demonstrate the usefulness of the technique.

The forced response results show a peak in the 1-1.5k.Hz range corresponding to modes at 1047Hz (fig.6), 1146Hz and 1282Hz, each of which involve significant input housing flexure. The bending stiffness of this component was therefore increased (by a factor of 2.25) by a simple adjustment to the model (reducing shaft bore by about 15%), and the modal and forced response recalculated. The response of the input casing (out-of-shaft plane) and the normal relative mesh displacement are shown in figs.13 and 14. The predicted casing response shows an attenuation of approximately 10dB over a wide frequency range, but at the expense of a slight increase in dynamic tooth load at about 1150Hz.

7. CONCLUSIONS

The characteristics predicted by this model have yet to be experimentally validated, although preliminary measurements indicate that the results are of the correct order of magnitude and order of complexity. The essential features predicted for the spiral bevel gearbox studies are:-

i) a wide scattering of natural frequencies occurs over the frequency range of interest, only a few of which are prone to gear error excitation

ii) over most of the frequency range severe coupling between components occurs which suggests that detailed analysis or measurements of individual component behaviour is not justified, except perhaps for low frequency problems, and localised phenomena such as shaft whip and local panel resonances,

iii) at typical operating conditions dynamic bearing loads of about 5% static load, and dynamic tooth loads of about 3% static load are predicted. Power transmitted can be quite high, so that these small percentage dynamic loads can represent a large amount of energy which can reduce component lives significantly and produce high levels of noise at discrete frequencies,

iv) the limited parametric study demonstrates the power of an economical mathematical model in reducing vibration amplitudes at the design stage. Localised manipulation of mass or stiffness can be expected to move resonances away from forcing frequencies, or modify mode shapes to extend component lives and reduce noise transmission. This can only reasonably be done at the design stage with an effective model,

v) before undertaking extensive parametric studies or extending the model to more complex gearboxes it will be necessary to perform the planned validation tests on a spiral bevel gearbox. Such testing must include measurement of modal response and transmission error,

vi) the analysis and limited validation suggests that more complex models may not be warranted.

8. REFERENCES

1. J.S. Pollard, Helicopter Gear Noise and its Transmission to the Cabin, 3rd European Rotorcraft and Powered Lift Forum, Paper No.52. Sept. 1977

2. S.L. Harris, Dynamic Loads on the Teeth of Spur Gears, Proc. I.Mech.E. 172, 87, 1958.

3. H. Opitz, Dynamic Behaviour of Spur and Helical Gears, J.S.M.E. Symp. Tokyo, Sept. 1967.

4. G.V. Tordion and H. Gerardin, Dynamic Measurements of the Transmission Error in Gears. J.S.M.E. Symp. Tokyo. Sept. 1967.

5. R.H. Badgley and R.M. Hartman, Gearbox Noise Reduction: Prediction and Measurement of Mesh Frequency Vibrations in a Helicopter Gearbox. Trans. ASME, B, V.96, 2, 567, May 1974.

6. M. Taha, C. Ettles, and P. Macpherson, Rigidity and Performance of a Helicopter Gearbox Assembly with Cantilevered Housing and Two Taper Roller Bearings. To be presented at Intl. Gear Conf., Chicago, Sept. 1977.

TABLE 1 - See p.50-7

TABLE 2 - TORSIONAL FREQUENCIES

Torsional Natural Freq. (Hz)	Overall system Natural Freq. (Hz).	Description
281	247 338	First order windup on couplings
1.30k	1.28k	Second order windup on couplings
1.51k	1.38k 1.75k	First order shaft torsion
3.08k	2.30k 2.70k 3.27k	Second order shaft torsion with severe tooth defl.
3.47k	3.48k	Third order shaft torsion

TABLE 1 - Predicted Natural Frequencies and Normal Modes

Mode deflections normalised to give largest single value of unity for each mode.

+ Values greater than 1 may occur at the mesh point because it is not one of the model nodes.

Node No.	Nat. Freq. (Hz)	Largest component Node and direction	Tooth Rel. Motion Normal	Sliding	Max. Torsional Coord. Node and Direction	Value	Assumed Modal Q-factor	Mode shape
1	121	4x	.00	.05	13θy	.00	20	In plane (xy) first order bending of output section
2	178	4z	.00	.00	13θy	.04	22	Out of plane (z) first order bending of output section
3	247	5z	.05	.16	13θy	.54	15	Torsional windup on couplings + out of plane bending of output section
4	338	10θx	.07	.22	10θx	1.00	15	Torsional windup on couplings + out of plane bending of output section (phase inversion wrt 3)
5	412	4x	.00	.68	10θx	.09	12	In plane first order overall mode with axial deflection of output section
6	719	5y	.01	.09	2θx	.04	8	Intermediate housing central node y deflection
7	779	5y	.04	.22	2θx	.12	12	Second order output section bending coupled xy, yz planes
8	832	9x	.08	1.84+	2θx	.22	9	Second order output section bending coupled xy, yz planes (phase invertion wrt 8)
9	1047	2z	.41	.72	2θx	.62	11	Input section bending coupled zy, xz planes
10	1133	5y	.00	.00	.00	.00	8	Intermediate housing central node y deflection
11	1146	2y	.03	.62	2θx	.04	11	Input section bending coupled xy, xz planes (phase inv. wrt 9)
12	1282	4θy	.50	.35	4θy	1.00	12	Input section bending coupled xy, xz planes. Second torsional windup on couplings.
13	1377	4θy	.20	.21	4θy	1.00	15	Severe third torsional. I/P section bending
14	1426	5z	.01	.06	4θy	.02	20	Out of plane defl. of intermediate housing central node.
15	1753	8θy	.20	.84	2θx	.13	13	Output section coupled complex bending. Nodes at WSB38 and WSB14.
16	1782	4θz	.08	1.55+	2θx	.06	10	Output section coupled complex bending. Nodes at WSB38 and WSB14. Predominantly inplane
17	1856	10y	.02	1.36+	2θx	.01	14	Axial deflection output shaft in opposition to output housing. Pinion xy bending.
18	1875	4θx	.01	.04	2θx	.00	16	Output shaft out of plane severe bending between WSB38 and WSB14.
19	1909	10y	.04	1.54+	2θx	.02	11	Complex coupled mode of input and output. Significant bearing deflections.
20	1956	2θx	.11	1.26+	2θx	.07	8	Complex coupled mode. Axial and bending deflection of pinion.
21	2161	10y	.41	.63	2θx	.27	11	Complex coupled mode - mainly in plane. Significant bearing deflections.
22	2297	2x	1.31	.88	2θx	.96	10	4th torsional mode. xy, xz bending and axial deflection of pinion.
23	2499	10z	.66	.36	2θx	.67	15	Complex out of plane bending on output housing and shaft. Torsional.
24	2552	4y	.03	.47	2θx	.04	14	Almost pure axial of output shaft and housing
25	2679	10z	.34	.20	2θx	.80	15	Pinion torsion. Complex out of plane deflections.
26	2822	8y	.02	1.17+	10θx	.08	11	Complex in plane on output and severe axial deflection of output
27	3127	8y	.34	.57	10θx	.24	12	In plane complex distortion. Out of plane of intermediate hsg - central node.
28	3240	5z	.00	.00	-	.00	8	Almost pure z deflection of intermediate housing central node.
29	3265	5z	.85	.77	10θx	.45	14	z deflection of node 5. High order torsion.
30	3477	9θy	.33	.38	9θy	1.00	20	Very pure high order torsional.
31	3668	8θx	.05	.09	10θx	.01	17	Out of plane bending of the output casing between WSB38 and WSB14.
32	3693	8θz	.20	.07	10θx	.06	17	In plane
33	3848	10θy	.12	.62	10θx	.03	12	Complex distortion of input housing and pinion.
34	4107	10θz	2.04+	.91	6θx	.42	10	Complex distortion of input housing and pinion. Significant high order torsion.
35	4115	10θx	.67	.27	6θx	.14	16	Input-output complex bending.
36	4359	9θx	.18	.07	10θx	.03	18	Input-output complex bending. Severe output shaftbending between WSB38 and WSB14.
37	4370	9θz	.13	.06	10θx	.02	18	Input-output complex bending. Severe output shaft bending between WSB38 and WSB14.
38	4975	11θy	.16	.49	6θx	.02	12	Input-output complex bending.
39	4998	12z	1.04+	.48	6θx	.13	12	Input-output complex bending.

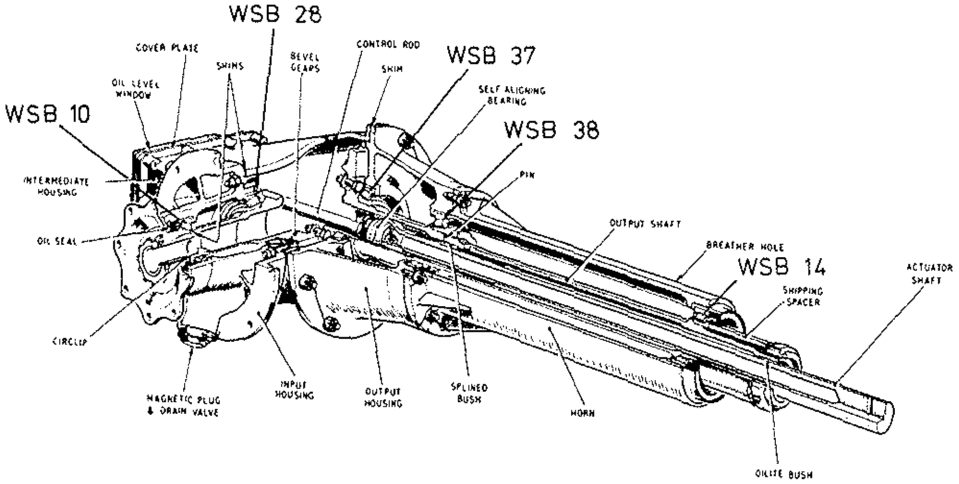

FIGURE 1 WESSEX TAIL ROTOR GEARBOX

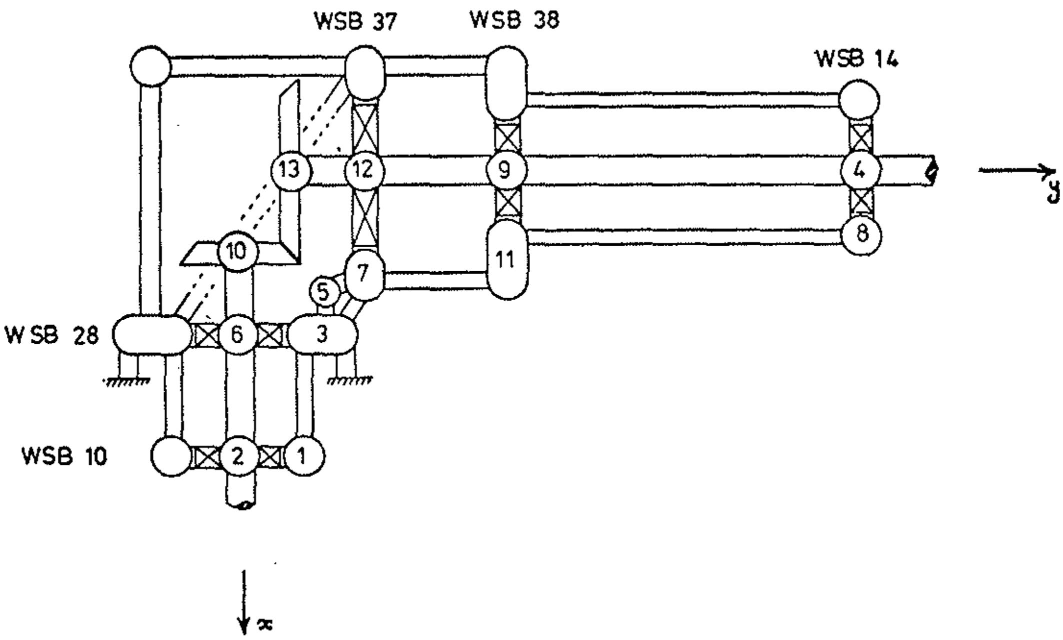

FIGURE 2 MODEL IDEALIZATION AND NODE NUMBERING.

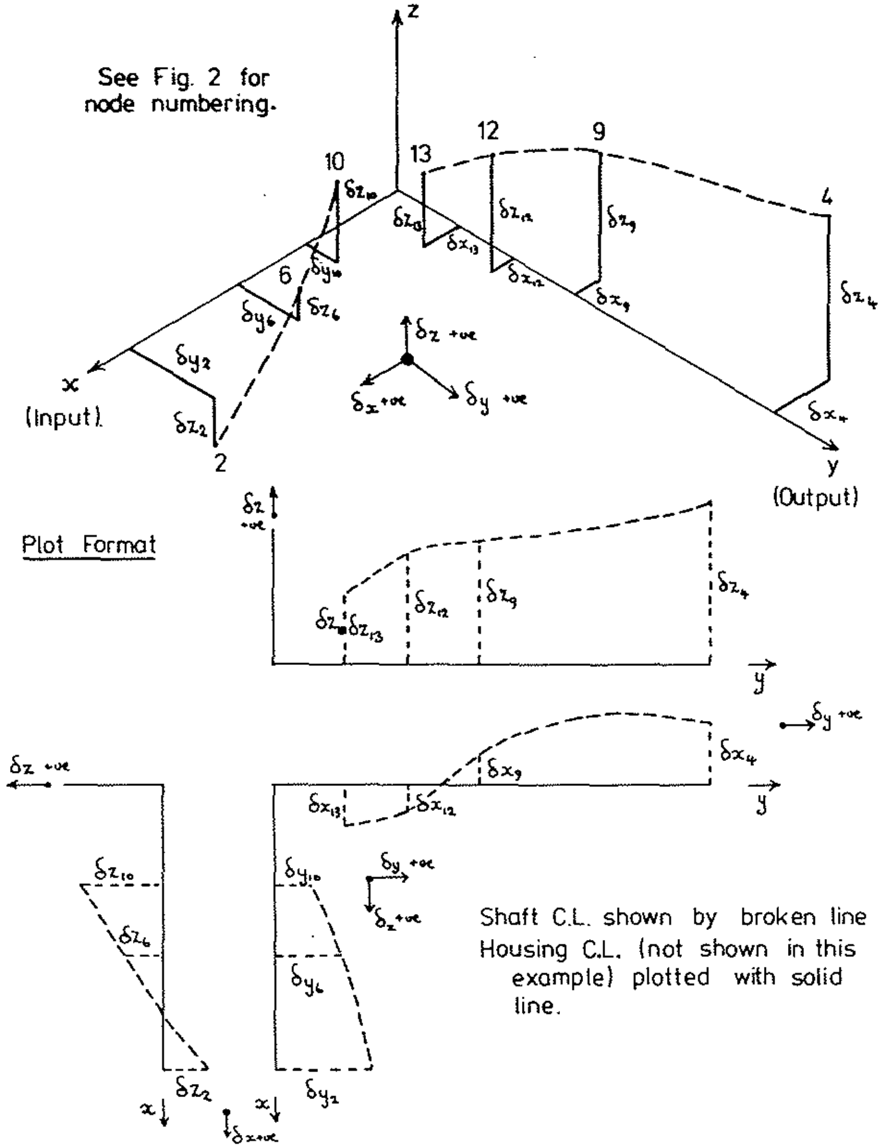

FIGURE 3 EXPLANATION OF PLOT AXES AND CONVENTIONS USED IN DEFLECTION & MODE PLOTS - FIGS. 4-7.

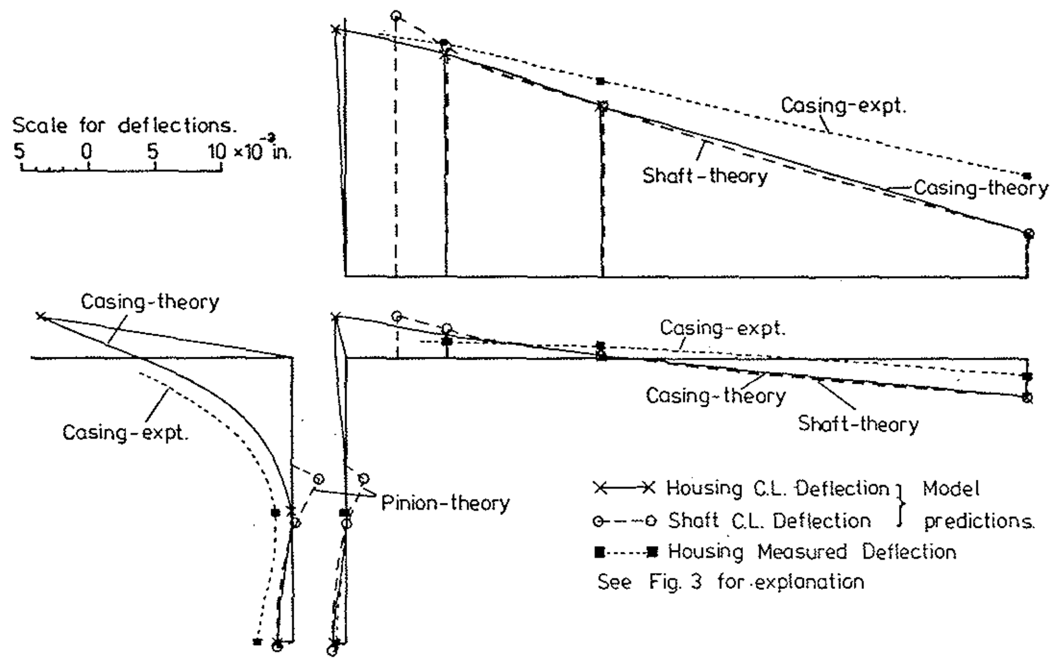

FIGURE 4 PREDICTED AND MEASURED DEFLECTIONS UNDER 4500 LBF-IN TORQUE (I/P).

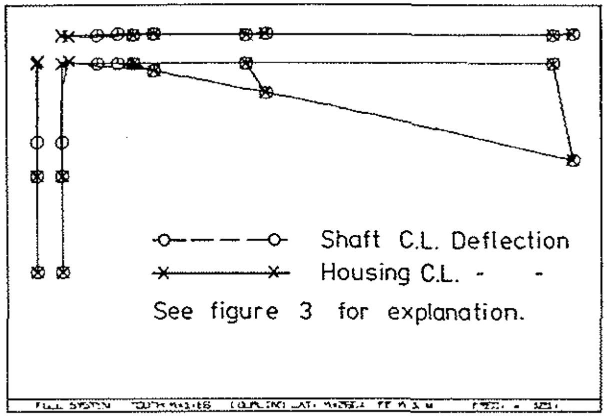

FIGURE 5 PREDICTED MODE SHAPE 121 Hz.

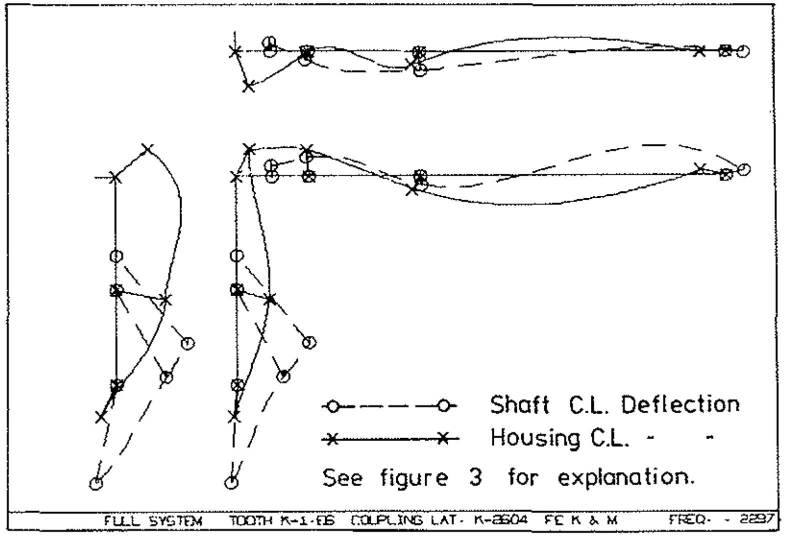

FIGURE 7 PREDICTED MODE SHAPE 2297 Hz.

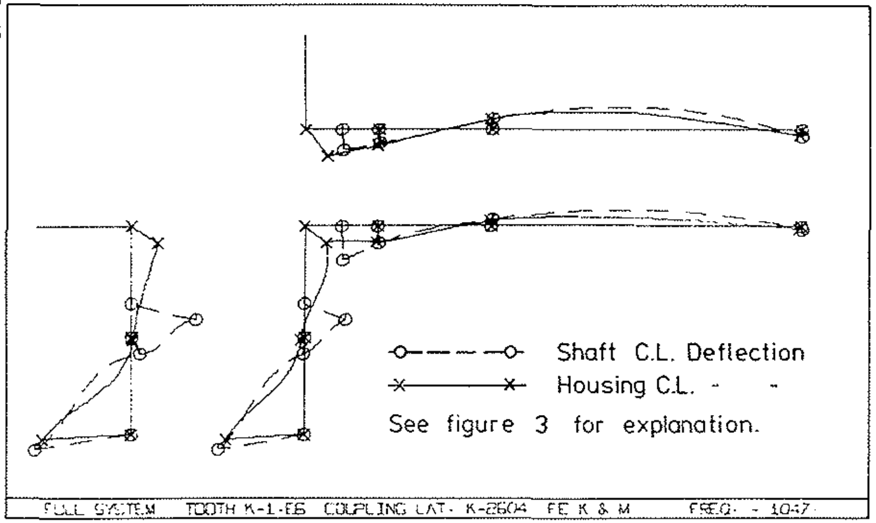

FIGURE 6 PREDICTED MODE SHAPE 1047 Hz.

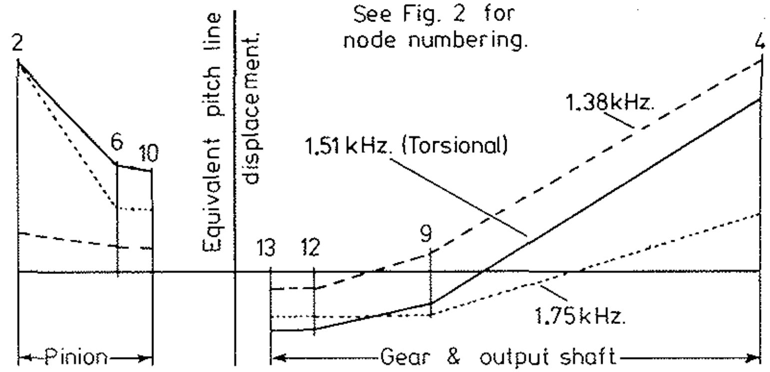

FIGURE 8 1.51 kHz. TORSIONAL MODE WITH COMPARABLE OVERALL SYSTEM MODES

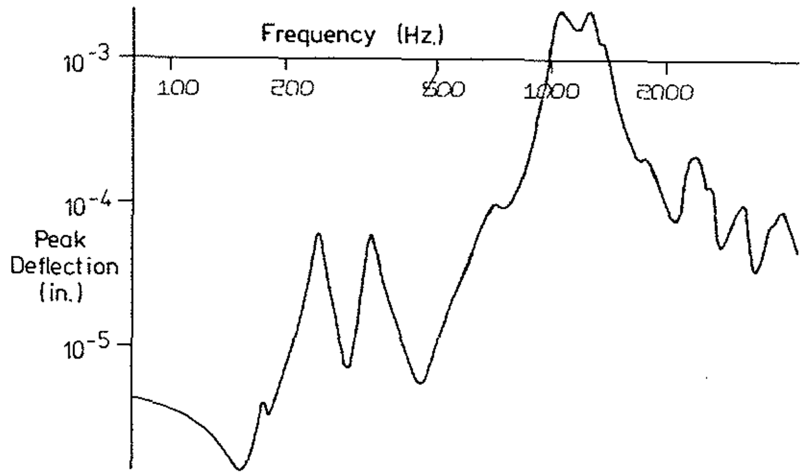

FIGURE 9 FORCED RESPONSE TO .001 IN. NORMAL MESH ERROR ON CASING OUT OF PLANE AT WSB 10 (1z)

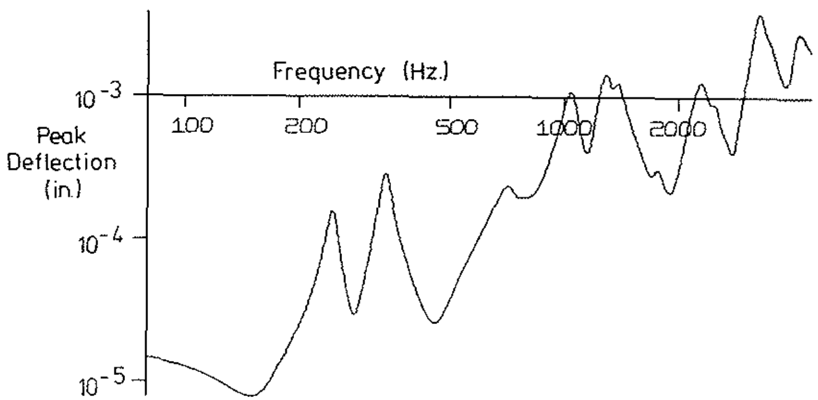

FIGURE 10 FORCED RESPONSE TO .001 IN. NORMAL MESH ERROR NORMAL RELATIVE MESH DISPLACEMENT.

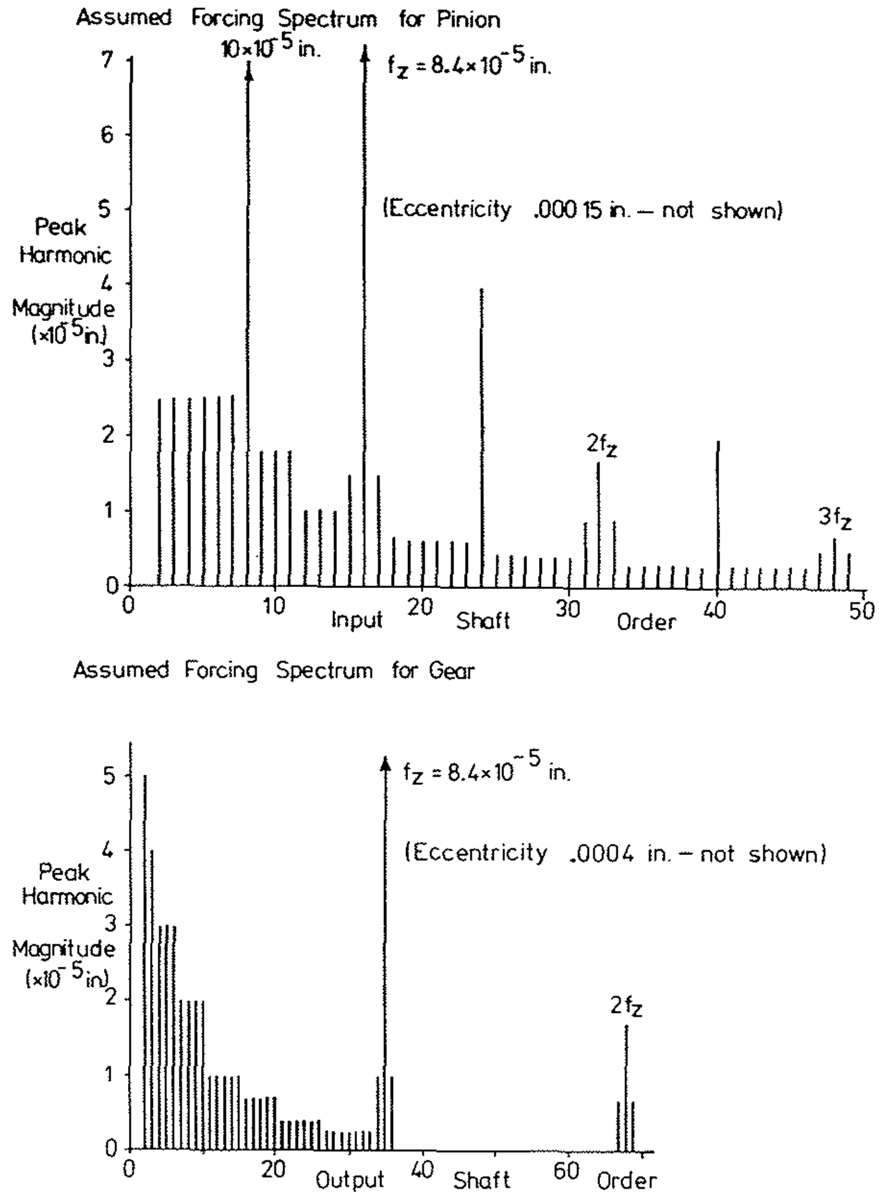

FIGURE 11 ASSUMED EXCITATION SPECTRA

(a) Predicted Spectrum – Out of plane on casing at WSB37 (7z)

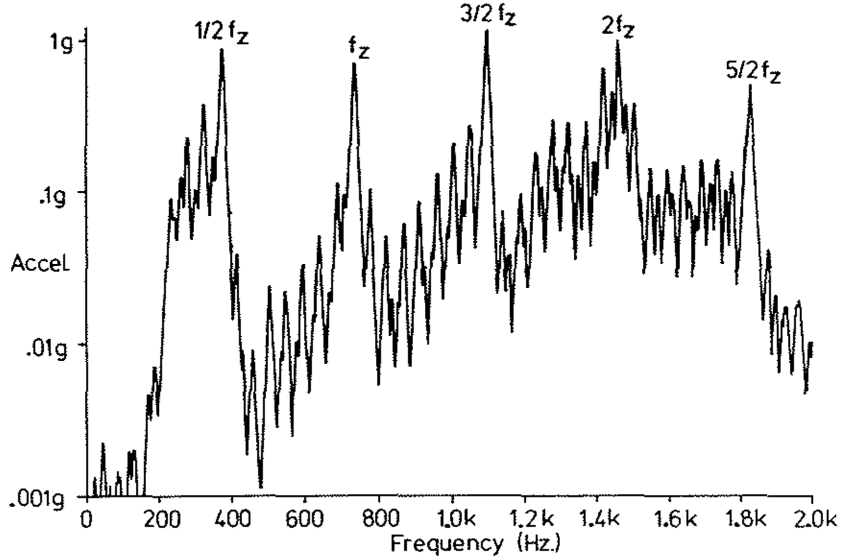

(b) Measured Spectrum — On casing at intermediate/output housing interface — 140 H.P.

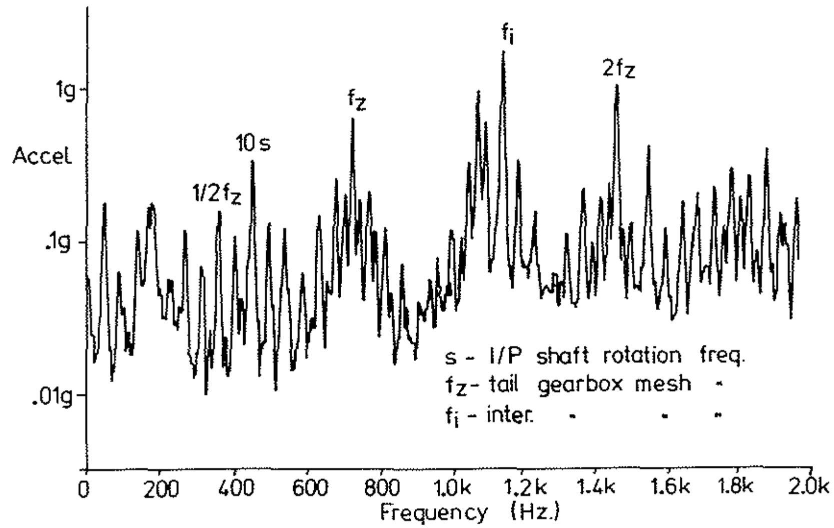

FIGURE 12 PREDICTED & MEASURED SPECTRA – 2730 R.P.M.

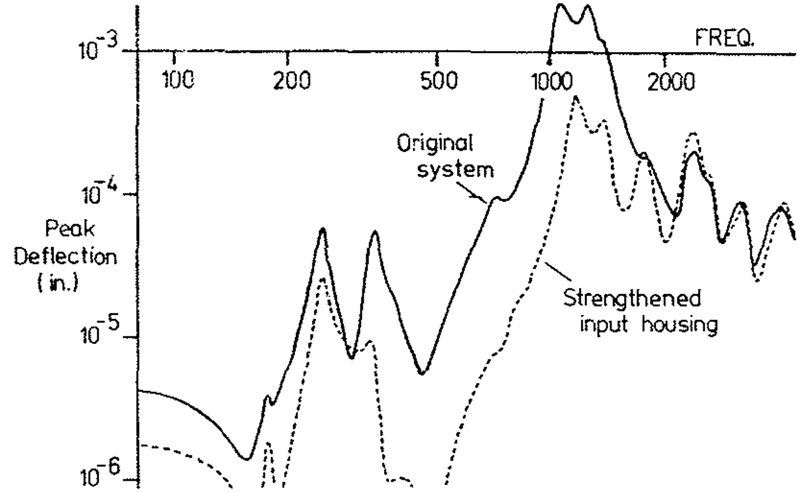

FIGURE 13 FORCED RESPONSE TO .001 IN. NORMAL MESH ERROR ON CASING AT WSB10 OUT OF SHAFT PLANE (1z).

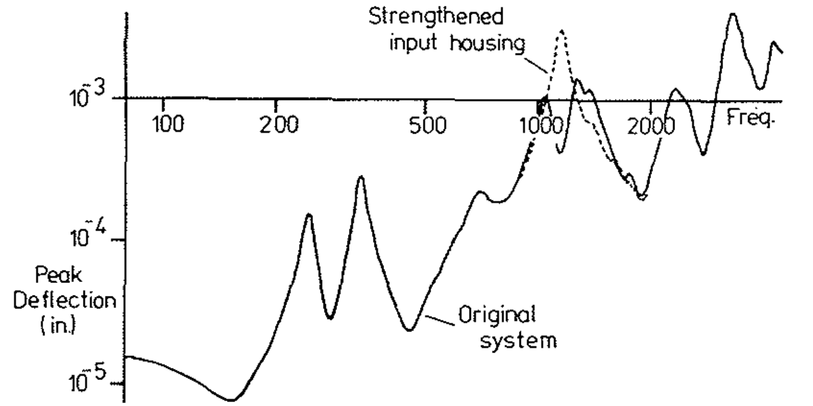

FIGURE 14 FORCED RESPONSE TO .001 IN. NORMAL MESH ERROR NORMAL RELATIVE MESH DISPLACEMENT.